

## Surface energies of Body-Centre-Cubic Metals: the Embedded Atom Method

F. Matthew-Ojelabi, A.A. Agbadaola, J. Adu, G.E. Adesakin and O.O. Odeyemi

Department of Physics, Ekiti State University, P.M.B 5363, Ado Ekiti, Ekiti State. Nigeria.

### Abstract

*This paper extends the embedding energy function  $F(\rho)$  developed by our group in earlier works to the compilation of the surface energies for low index facets of twelve bcc metals in the framework of the embedded atom method (EAM). The goal is to use the mathematical techniques for  $F(\rho)$ , which have hitherto worked for fcc metals, to generate a consistent database for bcc metallic elements. The  $F(\rho)$  parameters are obtained through a fit to the experimental mono-vacancy formation energy of each metal and are subsequently applied to the surface energy ( $\Gamma(hkl)$ ) calculation. These techniques make basic functions computationally simple and produce results with improved accuracy and reliability. The surface energies of the twelve metals considered generally do not follow the broken-bond model's trend  $\Gamma(100) > \Gamma(110)$  expected for bcc metals while  $\Gamma(100) > \Gamma(111)$  contrary to expectation. The accuracy of the calculated surface energy for each metal is reasonably good compared to existing theoretical data with similar background and experiments.*

**Keywords:** Embedded Atom Method (EAM), Embedding Energy Function ( $F(\rho)$ ), Body Centre Cubic (bcc) metals, Monovacancy Formation Energy, Surface Energy

### 1.0 Introduction

The surface energy is a vital electronic property of a metallic surface. Its theoretical knowledge is of great importance to understanding varieties of surface activities. Thus, it is important that any theoretical model [1-13] used in computer simulation of surface properties should, at least, predict accurately the surface relaxation and vacancy formation energy for low index surfaces of metallic elements.

To date, many of the existing atomistic simulation models have not given optimal performance in predicting the surface properties of bcc metals. Wilson and Riffe [12] partly ascribed the ineffectiveness of some of these models to longer range and angular nature of the forces in the less closed packed bcc lattice since these models worked better for fcc metals. In addition and most importantly, lack of desired success on the part of EAM has always been known to be due to the use of inconsistent experimental parameters as input on one hand and as yardstick for comparison of theoretical data on the other hand.

The embedded atom method (EAM) initiated by Daw and Baskes [2] is still the most widely applied interatomic potential for pure metals and alloys. EAM potential contains a many-body and a pairwise potential interaction terms intended to model the effective environment of an embedded atom. A heuristic derivation based on the concept of a local density [2] led to

$$E_{tot} = \sum_i F_i \left( \sum_{j \neq i} \rho_j(r_{ij}) \right) + \frac{1}{2} \sum_{\substack{i,j \\ j \neq i}} \phi_{ij}(r_{ij}) \quad (1)$$

$F(\rho)$  is the embedding energy function,  $\rho$  is the spherically averaged atomic density and  $\phi$  is an electrostatic two-body interaction. The host electron-density, assumed to be a linear superposition of contributions from individual atoms, is defined through;

---

Corresponding author: F. Matthew-Ojelabi, E-mail: fadekematthew@yahoo.com, Tel.: +2348030641917

$$\rho = \sum_{j \neq i} \rho_j(r_{ij}) \quad (2)$$

Eq.(1), known for computational simplicity, adequately caters for defects and other physical phenomena in solid or liquid state of metal. So far, it features three important functions which are  $F(\rho)$ ,  $\rho(r)$  and  $\phi(r)$ . The physical idea of measuring the electron density coming from atoms works probably because it is a very good measure of the number of states to be delocalized over.

One of the objectives of this manuscript is to show that the idea of EAM [2] for various crystal structures, founded on strong physical argument with few model parameters, produces results which are sometimes better than those offered by different modified versions of EAM with complicated  $F(\rho)$  and too many model parameters. Thus, the motivation for the construction of our  $F(\rho)$  in Matthew-Ojelabi et al [7] was computational simplicity leading to enhanced accuracy.

The rest of the paper is organized as follows: Section 2 surveys briefly the physical theoretical requirements for the present exercise. The calculation procedures are outlined in section 3 while the results of findings are presented in section 4. Section 5 concludes the work.

## 2.0 Theory

Crystals inherently possess imperfections sometimes called crystalline defects. A defect in which an atom is missing from one of the lattice sites is known as a vacancy. Vacancies occur naturally in all crystalline materials at any given temperature up to the melting points of the materials. Vacancies are formed during solidification due to vibration of atoms, local rearrangement of atoms, plastic deformation and ionic bombardments and so on leading to the formation of the simplest point defects. Vacancy is the dominant mechanism behind atomic transport in most elemental crystals and it is of fundamental importance in solid and surface science. Vacancies have also been known to play important role for surface morphology [9].

Given the importance of vacancies and parameters of energy at low temperature, the calculations of formation energies have become the regular subject of theoretical studies. The creation of a vacancy may be modeled by taking into consideration the energy required to break the bonds between an atom inside the crystal and its nearest neighbours. Once that atom is removed from the lattice site, it is put back on the surface of the crystal and some energy is retrieved because new bonds are established with other atoms on the surface. Yet, there is a net input of energy because there are fewer bonds between surface atoms than between atoms in the interior of the crystal. The simulation procedures for vacancy formation energy are outlined in this work as follows:

- Create a perfect crystal.
- Remove an atom.
- Relax the system using  $F(\rho)$ .
- Evaluate the potential energy of the system.
- Obtain the vacancy formation energy for different metals.

However, the calculation of the vacancy formation energy  $E_{mv}$  depends on the definition one proposes for it. From this point, our definition of the vacancy formation energy shall be based on how much cohesive energy is needed to form a vacancy. If the cohesive energy is negative, then certain energy is released when forming the vacancy. The Cohesive energy  $E_C$  can be defined as the interatomic potential energy per atom at the most stable state of the metal. It should be mentioned in passing that the vacancy formation energy is independent of the position of a vacancy.

We shall assume that the total potential energy, say  $E_i$  in the perfect crystal has reached the cohesive level and so does energy  $E_{vac}$  in the deformed structure after relaxation. Therefore, the monovacancy formation energy which is the energy to remove an atom and place it on the surface of that metal can be defined as

$$E_{mv} = E_C^{VACANCY} - E_C^{PERFECT} \quad (3)$$

where

$$E_C^{PERFECT} = \sum_i^N E_i = N E_C \quad (4)$$

$$E_C^{VACANCY} = (N - Z)E_C + Z E_C^{RELAXED} \quad (5)$$

Here,  $N$  is the number of atoms in the simulation cell and  $Z$  is the coordination number. For *bcc* metals,  $Z = 8$  such that

$$\begin{aligned} E_{mv} &= (N - 8)E_C + 8E_C^{RELAXED} - N E_C \\ &= -8E_C + 8E_C^{RELAXED} \end{aligned} \quad (6)$$

What really happens when a vacancy is formed is more than just removing an atom from the perfect crystal as demonstrated above. Rather, it is more or less like a rearrangement of atoms within the crystal, with the number of atoms kept constant as demonstrated in

$$E_c^{RELAXED} = (N - 8) \left[ F\left(\frac{8}{8}\rho_0\right) + \frac{1}{2} \times 8\phi_0 \right] + 8 \left[ F\left(\frac{7}{8}\rho_0\right) + \frac{1}{2} \times 7\phi_0 \right] \quad (7)$$

Once the vacancy formation energy is understood, one can channel its knowledge towards obtaining the surface energies via  $F(\rho)$ . In all cases, our calculations (of the surface energies) depend strongly upon the experimental vacancy formation energy used.

Concisely, the definition of the cohesive energy as function of  $F(\rho)$  is given as [2,4,5].

$$E_\eta = F\left(\frac{\eta}{Z}\rho_0\right) + \frac{\eta}{Z}\Phi \quad (8)$$

where  $\eta$  is the number of atoms before or after formation of vacancies and  $Z$  is the coordination number. The pair potential energy term is

$$\Phi = \frac{1}{2} \sum_{i,j} \phi(r_{ij}) \quad (9)$$

For the perfect crystal,

$$\Phi = \frac{1}{2} \times 8\phi_0 \quad (10)$$

Matthew-Ojelabi et al [7, 8] reported an embedding energy function of form

$$F(\rho) = AE_0 \left(\frac{\rho}{\rho_0}\right)^{q_1} - AE_0 \left(\frac{\rho}{\rho_0}\right)^{q_2} \ln\left(\frac{\rho}{\rho_0}\right) \quad (11)$$

Where  $A$ ,  $q_1$  and  $q_2$  are the adjustable parameters. The derivation of Eq.(11) was based on a simplified elastic energy expansion in Taylor's series via small displacements and in tandem with the local density  $\rho$  leading to a second-order ordinary differential equation in  $F(\rho)$ . Eq.(11), though simple, contains the basic physical character of the embedded atom method and provides another means of studying the functional dependence of the model using empirical data. It can also take care of those metals having negative Cauchy pressure.

In the current work we report the results of the calculations of the surface energies performed using Eq.(11) for twelve monatomic *bcc* metals. The present effort also targets a review of the concept of EAM and to subject Eq.(11) to further validity test having successfully applied it to *fcc* metals in earlier endeavours [7, 8]. It should be mentioned here that the simplification of the basic terminologies are intended for informative reasons.

Eq.(11) is the dominant tool for the present calculation where  $A$ ,  $q_1$  and  $q_2$  are the adjustable parameters,  $\rho_0$  is the equilibrium value of the local density. Note that  $\rho(r_0) = \rho_0$  and  $\phi(r_0) = \phi_0$ ,  $F(\rho_0) = AE_0 = E_c - \phi_0$  and  $F(0) = 0$  where  $E_0 = -E_c$  is the total or sublimation energy. For nearest-neighbour contribution in *bcc* metals, we must have

$$\sum \rho(r_i) = 8\rho_0 \quad (12)$$

### 3.0 Calculation Procedures

The calculations are in stages:

#### i. Monovacancy formation energy

Structural relaxation is a local effect. The energies of monovacancy and planar-surface formations for metals are dominated by the contributions before relaxation. Removing an atom draws neighbouring atoms toward the vacancy. The relaxation is significant for the first atoms but small already for the second and third shell of atoms surrounding the vacancy. The monovacancy formation energy is readily calculated for *bcc* metals using Eqs.(6-8) such that

$$E_8 = F\left(\frac{8}{8}\rho_0\right) + \frac{8}{8}\Phi = F(\rho_0) + \Phi = E_c \text{ and } \Phi = (1 + A)E_c \quad (13)$$

$$E_7 = F\left(\frac{7}{8}\rho_0\right) + \frac{7}{8}\Phi \quad (14)$$

Thus,

$$E_{mv} = -8F(\rho_0) + 8F\left(\frac{7}{8}\rho_0\right) - \Phi = 8F\left(\frac{7}{8}\rho_0\right) + (7A - 1)E_c \quad (15)$$

#### ii. Embedding energy function

The general expression for the embedding energy function (Eq.(11)) when  $\rho = \frac{n}{Z}\rho_0$  is

$$F\left[\left(\frac{Z-n}{Z}\right)\rho_0\right] = F\left[\left(1 - \frac{n}{Z}\right)\rho_0\right] = AE_0 \left\{ \left(1 - \frac{n}{Z}\right)^{q_1} - AE_0 \left(1 - \frac{n}{Z}\right)^{q_2} \ln\left(1 - \frac{n}{Z}\right) \right\} \quad (16)$$

$$= AE_0 \left\{ \begin{array}{l} 1 + \frac{n}{Z} S_1 - \frac{n}{Z} S_1 q_1 + \frac{1}{2} \left(\frac{n}{Z}\right)^2 S_2 q_1^2 - \frac{1}{6} \left(\frac{n}{Z}\right)^3 S_3 q_1^3 + \frac{1}{12} \left(\frac{n}{Z}\right)^4 S_4 q_1^4 \\ - \frac{1}{120} \left(\frac{n}{Z}\right)^5 q_1^5 - \left(\frac{n}{Z}\right)^2 S_1^2 q_2 + \frac{1}{2} \left(\frac{n}{Z}\right)^3 S_1 S_2 q_2^2 - \frac{1}{6} \left(\frac{n}{Z}\right)^4 S_1 S_3 q_2^3 \\ + \frac{1}{12} \left(\frac{n}{Z}\right)^5 S_1 S_4 q_2^4 - \frac{1}{120} \left(\frac{n}{Z}\right)^6 S_1 q_2^5 \end{array} \right\} \quad (17)$$

where

$$S_1 = 1 + \frac{1}{2} \left(\frac{n}{Z}\right) + \frac{1}{3} \left(\frac{n}{Z}\right)^2 + \frac{1}{4} \left(\frac{n}{Z}\right)^3 + \frac{1}{5} \left(\frac{n}{Z}\right)^4 + \dots \quad (18)$$

$$S_2 = 1 + \left(\frac{n}{Z}\right) + \frac{11}{12} \left(\frac{n}{Z}\right)^2 + \frac{5}{6} \left(\frac{n}{Z}\right)^3 + \dots \quad (19)$$

$$S_3 = 1 + \frac{3}{2} \left(\frac{n}{Z}\right) + \frac{7}{4} \left(\frac{n}{Z}\right)^2 + \dots \quad (20)$$

$$S_4 = \frac{1}{2} + \frac{n}{Z} + \dots \quad (21)$$

We used the following series expansions in Eq.(16) to obtain Eq.(17):

$$\ln(1 + x) = x - \frac{x^2}{2} + \frac{x^3}{3} - \dots \quad (22)$$

and (binomial expansion)

$$(1 + x)^n = 1 + \frac{nx}{1!} + \frac{n(n-1)x^2}{2!} + \dots \quad (23)$$

Thus, for  $Z = 8$  we have

$$F\left(\frac{8}{8}\rho_0\right) = F(\rho_0) = -AE_C \quad (24)$$

$$F\left(\frac{7}{8}\rho_0\right) = F\left[\left(1 - \frac{1}{8}\right)\rho_0\right] \quad (25)$$

$$F\left(\frac{6}{8}\rho_0\right) = F\left[\left(1 - \frac{2}{8}\right)\rho_0\right] \quad (26)$$

$$F\left(\frac{4}{8}\rho_0\right) = F\left[\left(1 - \frac{4}{8}\right)\rho_0\right] \quad (27)$$

The monovacancy formation energy of Eq.(15) can be calculated if  $q_1, q_2$  and  $A$  are known.

### iii. Surface energies

The surface energies along special directions are:

$$\Gamma_{100} = \frac{1}{a^2} (E_7 - E_8) = \frac{2}{a^2} \left\{ F\left(\frac{7}{8}\rho_0\right) + \frac{1}{8}(7A - 1)E_C \right\} \quad (28)$$

$$\Gamma_{110} = \frac{\sqrt{2}}{a^2} (E_6 - E_8) = \frac{\sqrt{2}}{a^2} \left\{ F\left(\frac{6}{8}\rho_0\right) + \frac{2}{8}(3A - 1)E_C \right\} \quad (29)$$

$$\Gamma_{111} = \frac{1}{a^2\sqrt{3}} (E_4 - E_8) = \frac{1}{a^2\sqrt{3}} \left\{ F\left(\frac{4}{8}\rho_0\right) + \frac{4}{8}(A - 1)E_C \right\} \quad (30)$$

### iv. Computational analysis

To test the reliability of Eq.(11) for *bcc* metals we obtained its parameters  $A, q_1$  and  $q_2$  through a fit of Eq.(15) to its experimental value.  $A, q_1$  and  $q_2$  were adjusted to match the experimental values of monovacancy formation energy  $E_{mv}$  and cohesive energy  $E_C$  for each metal considered. An essential aspect of the technique was the ability of our  $F(\rho)$ , within EAM, to reproduce the experimental value of the monovacancy formation energy by a simple and efficient procedure which utilizes a Fortran code based on Leipschl.com Force 2.0. Our *search* code was anchored on a very simple procedure which operated 1000 numerical grid points with spacing such that  $\Delta A = \Delta q_1 = \Delta q_2 = 10^{-6}$ . Thus, values of  $A, q_1$  and  $q_2$  which fitted Eq. (15) perfectly were obtained for each metal. The fitted values of  $A, q_1, q_2$  and other essential input parameters taken from Kittel [6] and Zhang et al [13] are listed in Table 1. The drawback of our algorithm is the existence of several potential minimal points. However, we made  $A < 1$  to avoid a not-physical situation and to ensure reliable and quick search.

## 4.0 Results and Discussion

The main results of this work are the surface energies of each metal along the three different orientations. The fitted values of  $A, q_1, q_2$  as well as the experimental values of the lattice constant  $a$  and cohesive energy  $E_C$  were used in Eqs.(28-30) to calculate the surface energies. For the surfaces of interest,  $n = 1, 2$  and  $4$  in Eq.(16 or 17). In Table 2, the results are compared to the data of first principles' study of Skriver and Rosengaard [10], modified embedded atom method (MEAM) of Baskes [1], the modified analytical embedded atom method (MAEAM) of Zhang et al [13] as well as the experimental (polycrystalline) data of deBoer et al [3] where available. Our approach gave a good description of the experimentally observed trends. The poorest agreement happens for the (111) facets for which we should have the lowest electron densities. The supposedly lowest-density surface was predicted to have lower surface energy than the closer-packed (100) planes surprisingly.

Though surface energy is readily compared to experiment, it should be stated that the comparison is, to a certain extent, challenging. The available experimental surface energies are fraught with impurities and are usually extrapolated to 0K. To date, the experimental data listed by deBoer et al [3] are the most reliable. The plot of the average of the selected calculated surface energies is compared to experiment [3] in Fig.1.

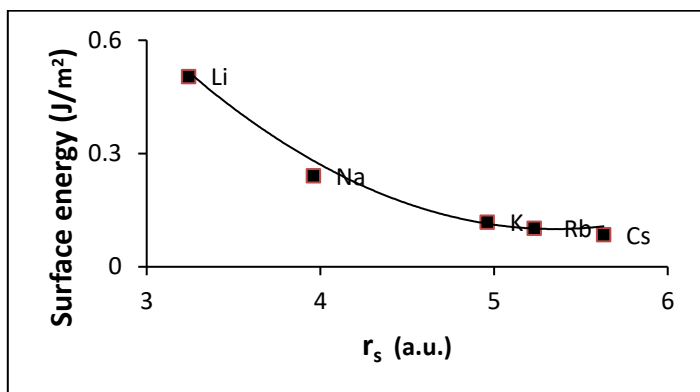


**Figure 1:** Calculated (average) surface energies of selected metals (solid squares) compared to a fit (solid line) of their polycrystalline values [3, 10].

**Table 1:** Model parameters of present work and experimental data of some *bcc* metals taken from Kittel [6] and Zhang et al [13].

Metal	$a$ (Å)	$E_{mv}$ (eV)	$E_c$ (eV)	$F(\rho)$ parameters		
				$A$	$q_1$	$q_2$
<i>Li</i>	3.5093	0.480	1.630	0.49465	5.44465	5.44465
<i>Na</i>	4.2096	0.340	1.113	0.50604	5.40604	5.20004
<i>K</i>	5.3210	0.340	0.934	0.52556	5.43156	5.25560
<i>Rb</i>	5.7030	0.341	0.852	0.47866	5.87660	5.30066
<i>Cs</i>	6.1410	0.322	0.804	0.46005	6.36005	5.19017
<i>Fe</i>	2.8664	1.790	4.280	0.46011	6.41010	5.41010
<i>V</i>	3.0282	2.100	5.310	0.40361	7.30361	5.30361
<i>Cr</i>	2.8846	1.600	4.100	0.42749	6.82748	5.20248
<i>Nb</i>	3.3007	2.750	7.570	0.40001	7.20002	5.20002
<i>Mo</i>	3.1468	3.100	6.820	0.42074	7.32174	5.19500
<i>W</i>	3.1650	3.950	8.900	0.40801	7.35801	6.20001
<i>Ta</i>	3.3026	2.950	8.100	0.40102	7.10102	5.70102

**Table 2:** Surface energies of twelve *bcc* metals of present work compared with the data of first principles' study of Skriver and Rosengaard [10], modified embedded atom method (MEAM) of Baskes [1] and the modified analytical embedded atom method (MAEAM) of Zhang et al [13] where available as well as the experimental data of deBoer et al [3].

Metal	Crystal Face ( <i>hkl</i> )	Surface energies in $J/m^2$				
		EAM Present Work	First Principles Calculations (Ref[10])	MEAM (Ref[1])	MAEAM (Ref[11])	Experiment (Ave) (Ref[3])
<i>Li</i>	(100)	0.6519	0.436	0.431	0.2693	0.525
	(110)	0.5583	0.458	0.202	0.2529	
	(111)	0.3030		0.279	0.3108	
<i>Na</i>	(100)	0.3193	0.236	0.288	0.1330	0.260
	(110)	0.2673	0.307	0.169	0.1247	
	(111)	0.1386		0.202	0.1535	
<i>K</i>	(100)	0.1767	0.129	0.182	0.0833	0.130
	(110)	0.1076	0.112	0.110	0.0781	
	(111)	0.0700	0.116	0.125	0.0961	
<i>Rb</i>	(100)	0.1232	0.107		0.0725	0.110
	(110)	0.1212	0.092		0.0680	
	(111)	0.0634	0.089		0.0836	
<i>Cs</i>	(100)	0.0947	0.092		0.0592	0.095
	(110)	0.1054	0.072		0.0555	
	(111)	0.0558	0.070		0.0683	
<i>Fe</i>	(100)	2.3137		2.289	1.537	2.480
	(110)	1.5990	2.660, 3.090	1.566	1.429	
	(111)	1.3820		1.720	1.772	
<i>V</i>	(100)	3.6650		2.490	1.705	2.550
	(110)	0.6906	2.020	1.705	1.548	
	(111)	1.9647		1.805	1.959	
<i>Cr</i>	(100)	1.9635		1.230	1.461	2.300
	(110)	0.7873	3.630	1.032	1.315	
	(111)	1.6593		1.247	1.677	
<i>Nb</i>	(100)	2.5092		2.788	1.995	2.700
	(110)	0.7956	1.640	1.868	1.767	
	(111)	2.2836		2.018	2.283	
<i>Mo</i>	(100)	2.6794		2.122	2.332	3.000
	(110)	1.0216	3.180	1.930	2.118	
	(111)	2.2926		1.861	2.679	
<i>W</i>	(100)	3.2981		2.646	2.882	3.680
	(110)	1.1260	3.840	2.232	2.638	
	(111)	3.1046		2.247	3.315	
<i>Ta</i>	(100)	3.2736		3.292	1.963	3.150
	(110)	1.5676	1.790	2.173	1.802	
	(111)	2.4155		2.305	2.259	

## 5.0 Conclusion

The main contribution of this paper is the extension of the embedding energy function of Eq.(11) to *bcc* metallic elements. The extension was anchored on the strong theoretical footing of the embedded atom method (EAM). The theoretical procedures were successfully carried out on *bcc* alkali and transition metals involving various bonding mechanisms, indicating that Eq.(11) could describe the elastic and simple defect properties of the various materials just as it has done for their *fcc* counterparts.

We performed the structural analysis and calculated the surface energies for different planar orientations and compared the results to experiments and other theoretical calculations. Our results are in reasonable agreement with experiment.

In contrast to most modified versions of EAM, our EAM type has a consistent analytical  $F(\rho)$  which requires just 3 fitting parameters and considers first-nearest neighbor interactions only. Extension of Eq.(11) to second-neighbour interactions for all crystalline structures including *hcp* is conceivable.

## 6.0 Acknowledgement

One of us (FM) is grateful to Professor J. O. A. Idiodi of Department of Physics, University of Benin, Benin-City, Nigeria for inspiration and support.

## 7.0 References

- [1] M. I. Baskes, Phys. Rev. B. 46, 5(1992) 2727-2742.
- [2] M. S. Daw, M. I. Baskes, Phys. Rev. B 29, 12 (1984) 6443-6453.
- [3] F. R. deBoer, R. Boom, W. C. M. Mattens, A. R. Miedema, A. R. and Niessen A., Cohesion in metals; Transition metal alloys, Fourth ed., North-Holland, Amsterdam (1988).
- [4] S. M. Foiles, M. I. Baskes, M. S. Daw, Phys. Rev. B, 33, 12 (1986) 7983-7991.
- [5] R. A. Johnson, Phys. Rev. B, 37, 8, (1988) 3924-3921.
- [6] C. Kittel, Introduction to Solid State Physics, Fifth ed., Wiley Eastern Limited, India, (1985), 31-74.
- [7] F. Matthew-Ojelabi, J. O. A. Idiodi, I. I. Ajibade and O. Enoch, J. Nig. Ass. Math. Phys. (NAMPA), 22(2012) 35-42.
- [8] F. Matthew-Ojelabi and I. I. Ajibade, J. Nig. Ass. Math. Phys. (NAMPA), 25 1 (2013) 37-42.
- [9] T. R. Mattsson and A. Mattsson, Phys. Rev. B, 66, 12 (2002) 214110(1)-214110(8).
- [10] H. L. Skriver and N. M. Rosengaard, Phys. Rev. B, 46, 11 (1992) 7157-7168.
- [11] Y. -N. Wen, J. -M. Zhang, Comp. Mat. Sci., 42 (2008) 282-297.
- [12] R. B. Wilson and D. M. Riffe, J. Phys.: Condens. Matter 24 (2012) 335401-335457.

- [13] J. -M. Zhang, Y. -N Wen and K. -W Xu, CEJP 4 (4) 2006 481-493.